Psychoneuroendocrinology 108 (2019) 163–171

Contents lists available at ScienceDirect

Psychoneuroendocrinology

journal homepage: www.elsevier.com/locate/psyneuen

Metabolic and endocrinal effects of N-desmethyl-olanzapine in mice with obesity: Implication for olanzapine-associated metabolic changes

Xueli Zhang[a,*], Yi Zhao[a], Hua Shao[a], Xiao Zheng[b,*]

[a] Department of Pharmacy, Zhongda Hospital, School of Medicine, Southeast University, Nanjing 210009, China
[b] Laboratory of Metabolism and Drug Target Discovery, State Key Laboratory of Natural Medicines, College of Pharmacy, China Pharmaceutical University, Nanjing 210009, China

ARTICLE INFO

Keywords:
N-desmethyl-olanzapine
Metabolic disturbance
Insulin resistance
Energy metabolism
Atypical antipsychotics

ABSTRACT

Clinical use of the antipsychotic drug olanzapine (OLA) is associated with metabolic side effects to variable degrees. N-desmethyl-olanzapine (DMO) is one major metabolite of OLA, but its potential involvement in the metabolic responses remains unclear. Here we examined whether DMO can directly impact the metabolic, endocrinal and inflammatory parameters under conditions of metabolic disturbance. DMO administration (2 mg/kg, i.g.) to high-fat diet induced obesity mice for 4 weeks induced a remarkable loss of body weight and fat mass. DMO improved insulin resistance and energy expenditure in mice, but had no significant effects on dyslipidemia or hepatic steatosis. Moreover, DMO induced morphological changes in the white adipose tissue, accompanied by reduced interleukin-1β (IL-1β) production and increased UCP1 expression. These findings demonstrate that DMO is devoid of the metabolic side effects commonly observed for OLA during obesity, which suggests that the N-desmethyl metabolism may function to regulate the metabolic responses to OLA.

1. Introduction

The advent of atypical antipsychotics (AAPs) represents a major therapeutic advance in the clinical management of schizophrenic or bipolar patients, attributed to a lower incidence of extrapyramidal side effects and better efficacy (Aringhieri et al., 2018). However, metabolic side effects, typically weight gain and insulin resistance, have become a serious concern in the clinical use of AAPs (Bobo et al., 2013). As a typical example, olanzapine (OLA) treatment of schizophrenia is associated with a high propensity for weight gain and metabolic disturbances in some patients (Irwin and Gault, 2013). Despite much progress in the past decade, the biological determinants of AAPs-associated metabolic responses remain incompletely understood. There is ample evidence that factors such as gender, age and life style may affect the magnitude and even occurrence of untoward metabolic effects among patients treated with OLA and other AAPs (Daurignac et al., 2015; Henderson et al., 2015; Musil et al., 2015; Yatham et al., 2016). Our previous study and others have also found pathophysiological-dependent effects of OLA on energy metabolism in animal models (Boyda et al., 2010; Davey et al., 2012; Horska et al., 2016; Townsend et al., 2018; Zhang et al., 2018).

Variable pharmacokinetic profile of OLA is commonly observed during clinical therapy (Castberg et al., 2017; Zabala et al., 2017). Studies have shown that the concentration variability of OLA only well correlate with its mental effects, but has a poor relevance to the adverse metabolic effects, suggesting the existence of other factors (Lu et al., 2016). In addition to the parent drug, recent studies are beginning to focus on the concentration of OLA metabolites in schizophrenia patients (Theisen et al., 2006; Lu et al., 2013, 2016). Indeed, ever since the drug discovery stage, it has been acknowledged that OLZ is extensively metabolized to several molecules such as 2-hydroxymethyl OLA and N-desmethyl-olanzapine (DMO) (Kassahun et al., 1997; Mattiuz et al., 1997). The potential involvement of OLA metabolites in the metabolic outcome to OLA therapy remains, however, largely unexplored. Very recently, a study in OLA-treated schizophrenia patients showed that the plasma concentration of DMO was negatively correlated with the metabolic disturbance (Lu et al., 2018). This is reminiscent of an earlier study reporting that glucose and insulin level of patients treated with OLA was inversely correlated with plasma DMO level (Lu et al., 2013). These findings raise an intriguing and open question as to the involvement of DMO in the metabolic disturbance after OLA administration.

The aim of this study was to investigate the direct impacts of DMO on metabolic and endocrinal parameters in a clinically-relevant context. Schizophrenia patients show metabolic disturbance to different degrees before and during OLA treatment (Chang et al., 2013). Therefore, we

* Corresponding authors.
E-mail addresses: xlzhang1225@126.com (X. Zhang), xzheng@cpu.edu.cn (X. Zheng).

https://doi.org/10.1016/j.psyneuen.2019.06.017
Received 5 May 2019; Received in revised form 26 June 2019; Accepted 28 June 2019

focused on the metabolic impacts of chronic DMO administration in mice with obesity, which feature clinically-relevant markers of metabolic disturbance. We examined the change in metabolic, endocrinal and inflammatory parameters at tissue and systemic level to explore the functional impacts of DMO in metabolic disturbance. The results indicate that elucidation of the metabolic and endocrinal actions of OLA metabolites such as DMO could provide novel insights into its clinical side effects.

2. Methods

2.1. Animals

Adult male C57BL/6 J mice were purchased from Vital River Laboratory Animal Co., Ltd (Beijing, China) and maintained in temperature (25℃) and humidity controlled conditions with 12-h light/dark cycles and free access to food and water. Animals were 5–6 weeks old and weighed between 18 and 20 g at the start of the study. After acclimation to the housing conditions, the animals were then fed with a high-fat diet (45% kcal fat, Trophic Animal Feed, Nantong, China) for 12 consecutive weeks to induce obesity. All experiments were approved by the Southeast University Animal Ethics Committee (Nanjing, China) and conducted in accordance with the National Institutes of Health Guide for the Care and Use of Laboratory Animals.

2.2. Drugs and administration

N-desmethyl-olanzapine (sc-208019, Santa Cruz, USA) was dissolved in pure water with pH adjustment by 1 M hydrochloric acid and orally administered to mice once daily (2 mg/kg). This dose was chosen based on a previous report of DMO administration in C57BL/6 mice and our preliminary study (Wiebelhaus et al., 2011). At the end of 8th week of high-fat diet, mice with clear signs of obesity were randomized into the vehicle group (HFD, n = 6) and the DMO treatment group (HFD + DMO, n = 7). Mice received oral administration of vehicle or DMO once daily during the following 4 weeks of the experimental period (9th to 12th week). Body weight and food intake were recorded every 2 days. Behavioral changes of mice, in particular sedation and locomotion activity, were also observed during this period. The experimental design is depicted in Fig.1

2.3. Glucose and insulin tolerance tests

The determination of glucose homeostasis and insulin sensitivity was performed in the 12th week according to the procedures previously described (Zhang et al., 2018). Briefly, for intraperitoneal glucose tolerance testing (IGTT), mice were fasted overnight and intraperitoneally given a single dose of D-glucose (2 g/kg), and blood glucose level was measured at different intervals (15, 30, 45, 60, 90, 120 min) with an UltraEasy glucometer (Johnson & Johnson, Shanghai, China). For insulin tolerance testing (ITT), mice were fasted for 4 h and intraperitoneally injected with recombinant human insulin (0.35 U/kg, WanBang Biomedical, Xuzhou, China). The change of blood glucose concentrations were expressed as percent of the baseline level.

2.4. Indirect calorimetry study

Indirect calorimetry study in mice were conducted as previously described with minor modifications (Choi et al., 2018). Before the start of recording, mice were housed individually and habituated to each chamber of an indirect calorimetry system (TSE systems, Beijing, China) for 12 h, provided with free access to food and water. Then, the oxygen consumption (VO_2) and carbon dioxide production (VCO_2) were monitored under a 12-h light, 12-h dark cycle with constant environmental temperature (22 ℃). The respiratory exchange ratio (RER) were calculated by the ratio of VCO_2/VO_2.

2.5. Rectal temperature measurement

A digital thermometer (Omron, Shanghai, China) was used for measurement of rectal temperature at around 4:00 p.m. in ambient temperature. The probe was gently inserted about 1˜2 cm into the anal ducts of mice, and care was made not to induce overt reactions of the animal.

2.6. Tissue histology

The mice were humanely sacrificed by isoflurane at the end of the 12th week. For the preparation of histological analysis, white adipose tissue at the inguinal, epididymal and perirenal sites, the interscapular brown fat and a lobe of liver were exercised and immediately fixed in 4% paraformaldehyde for 48 h. The samples were then paraffin embedded, cut into 5 μm thick sections and stained with hematoxylin-eosin using common protocols. To examine the lipid droplets in the liver, the same lobe of livers were collected at the sacrifice of mice and placed into dry ice before OCT embedding. The samples were then cut into 7 μm slices, and then stained for lipids using a standard Oil Red O (ORO, Merck, Germany) staining protocol. All the images were captured in a random manner under bright field mode of microscope (Leica, Germany). The average diameters of adipocytes in white adipose tissue were calculated with the Image J software.

2.7. Biochemical assay of serum

Serum levels of insulin, adiponectin and leptin were analyzed by commercially available ELISA kits (all purchased from Crystal Chem, IL,

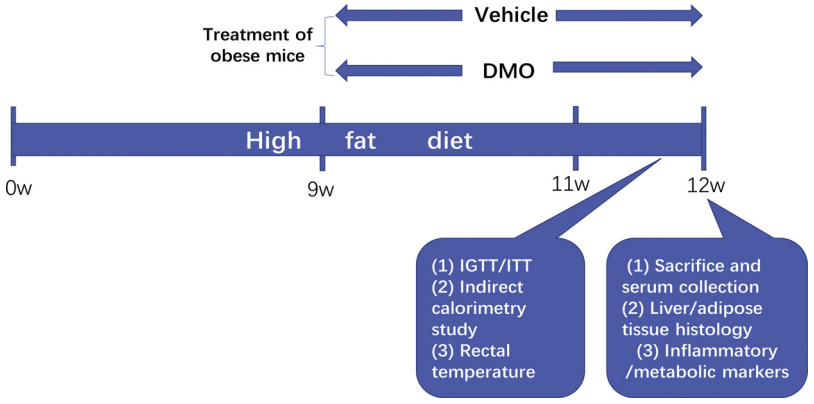

Fig. 1. Schematic illustration of the experimental design in mice. Mice received high-fat diet (HFD) during the whole study (12 weeks), and DMO treatment started from the 9th week (from the 9th to 12th week). IGTT, intraperitoneal glucose tolerance test, ITT, insulin tolerance test.

USA) following the instructions by the manufacturer. Serum levels of triglyceride (TG), total cholesterol (TC) and non-esterized fat acids (NEFA) were measured by commercially available kits (JianChen Biochem, Nanjing, China). The same method was also used for the determination of hepatic TG and TC following the manufacturer instructions. The calculation of Homeostasis model assessment (version 2, HOMA2-IR) is based on fasting blood glucose concentration and serum insulin level.

2.8. Western Blot analysis

The adipose tissues were excised on ice plates and homogenized with ice-cold RIPA lysis buffer (150 mM NaCl, 50 mM Tris, 0.5% sodium deoxycholate,1% Triton X-100) supplemented with protease/phosphatase inhibitors (all purchased from Beyotime Biotech, Nantong, China). After centrifuge at 13,000 *g* for 15 min, supernatants were collected and protein concentrations in the supernatants were measured using a commercially available BCA kit (Beyotime Biotech, Nantong, China). Protein samples were separated by SDS-PAGE and immunoblotted for UCP-1 (#23673-1-AP, 1:1000; Proteintech, Wuhan, China), IL-1β (#12242, 1:1000; Cell Signaling Technology, MA, USA) and β-actin (#AB0035,1:5000; Abways, China). The immunoreactive bands were visualized with HRP substrates using the Tanon 5200 imaging system (Tanon Sci & Tech, China). Densitometric analyses of the immunoblots were carried out by a built-in quantitative software (Tanon Sci & Tech, China) and relative band intensity compared to control group was used for statistical analysis.

2.9. Quantitative real-time PCR analysis

Total RNA extraction, reverse transcription and real-time PCR were performed as previously described by us (Zhang et al., 2018). The gene amplification was performed with SYBR Green and primer sequences (5′-3′) were as follows: *Il1β*, forward-GCAACTGTTCCTGAACTCAACT, reverse-ATCTTTTGGGGTCCGTCAACT; *Tnfα*, forward-GAGAGATTGGC TGCTGGAAC, reverse-TGGAGACCATGATGACCGTA; *Mcp1*, forward-GTGAAGTTGACCCGTAAA, reverse-TCCTACAGAAGTGCTTGA; *Cd68*, forward-TGTCTGATCTTGCTAGGACCG, reverse-GAGAGTAACGGCCTT TTTGTGA; *Gapdh,* forward-AGGTCGGTGTGAACGGATTTG; reverse-TGTAGACCATGTAGTTGAGGTCA. The fold change in gene expression was calculated by the $2^{-\triangle\triangle CT}$ method and Gapdh was used as the control.

2.10. Statistical analysis

Data are expressed as mean ± SEM. Statistical analyses were carried out with the SPSS software (version 18.0., IBM, USA). Analyses of significant differences between two groups were performed using two-tailed Student's *t*-test, A two-way repeated-measures ANOVA was used for analyzing body weight curve, IGTT and ITT, and the indirect calorimetry data, with Bonferroni *post hoc* test. Significance was accepted at $p < 0.05$.

3. Results

3.1. DMO decreases body weight and adiposity in obese mice

To simulate the metabolic disturbance observed in schizophrenia patients, mice were subjected to high-fat diet (HFD, 45% fat) to induce markers of obesity. At the end of 8th week, DMO was orally administered to mice that have shown typical markers of metabolic disturbance. The daily food intake was comparable between vehicle and DMO-treated mice (Fig.2A, $p > 0.05$ by Student's *t*-test). Also, no signs of behavioral changes such as sedation were observed after the chronic exposure to DMO (data not shown). Nevertheless, from the growth curves after DMO treatment, we observed a clear trend of DMO to slow down the body weight gain early since the 5th day of drug administration, which culminated in a significant decrease in body weight at the end of 4-week treatment (Fig.2B, $p < 0.05$ by two-way repeated-measures ANOVA).

After sacrifice, DMO-treated mice had much smaller body shape and adiposity by appearance (Fig.2C). In line with this, markedly reduced fat mass were found in all the white adipose tissue (WAT), including those in the inguinal ($p < 0.01$ by Student's *t*-test), epididymal ($p < 0.01$ by Student's *t*-test) and perirenal ($p < 0.001$ by Student's *t*-test) sites (Fig.2D). No significant change of brown adipose tissue (BAT) mass was found (Fig.2D, $p > 0.05$ by Student's *t*-test). In addition, compared to vehicle-treated counterparts, there is no obvious change of serum TG or TC of the DMO-treated mice (Fig.2E), although a significant decrease of NEFA could be observed after DMO treatment (Fig.2E, $p < 0.01$ by Student's *t*-test). Collectively, these findings provide preliminary evidence that DMO has the potential to counteract weight gain and adipose expansion in obesity.

3.2. DMO improves insulin sensitivity in obese mice

There are numerous reports that OLA may impair the metabolic actions of insulin (Irwin and Gault, 2013; Lord et al., 2017), but whether its metabolites are involved in this process is unknown. A typical metabolic change in obese mice is insulin resistance, which provides a clue for us to dissect the impact of DMO on this parameter. To this end, the obese mice were subjected to the intraperitoneal glucose tolerance test (IGTT) and insulin tolerance test (ITT), respectively. In comparison to vehicle-treated mice, DMO treatment showed no effect on the dynamics of blood glucose in the IGTT (Fig.3A; $p > 0.05$ by two-way repeated-measures ANOVA). Nevertheless, in the ITT, we observed a quick drop of the blood glucose after insulin injection (15 min) and much slower increase to baseline level in DMO-treated mice (Fig.3B, $p < 0.05$ by two-way repeated-measures ANOVA). Further determination of serum insulin and blood glucose showed that DMO-treated mice actually had low circulating insulin (Fig.3C, $p < 0.05$ by Student's *t*-test) and a much lower value of HOMA2-IR (Fig.3D, $p < 0.05$ by Student's *t*-test). Of interest, the serum level of adiponectin and leptin were comparable between vehicle and DMO-treated mice (Fig.3D, E, all $p > 0.05$ by Student's *t*-test). Taken together, these findings suggest that DMO could exert a mild alleviating effect on HFD-induced insulin resistance in mice.

3.3. DMO does not alleviate HFD-induced liver steatosis

As a typical change induced by HFD, the dysregulation of hepatic lipid metabolism contributes to impaired insulin response, liver steatosis and tissue injury (Petersen and Shulman, 2018). We therefore examined the potential impact of DMO on liver dysfunction of obese mice. No significant difference in liver weight was noted between DMO and vehicle-treated mice (Fig.4A, $p > 0.05$ by Student's *t*-test). Histological examination of the liver showed a massive injury of hepatocytes with markers of necrosis and inflammation, consistent of the detrimental effects of HFD on the liver. The liver from DMO-treated mice showed no histological improvement compared to the liver of vehicle-treatment counterparts (Fig. 4B). In further analysis with ORO staining, we found no obvious difference in the degree of lipid accumulation in the liver between the two groups of mice (Fig. 4C). In line with histological changes, neither hepatic TC nor TG was significantly different (Fig.4D, $p > 0.05$ by Student's *t*-test). These data indicate that DMO fails to improve hepatic injury and steatosis in the context of obesity.

3.4. DMO improves systemic energy metabolism of obese mice

Metabolic markers of obesity such as adipose accumulation and insulin resistance develop when the rate of energy input exceeds the rate of expenditure in a chronic manner. Previous reports on OLA-

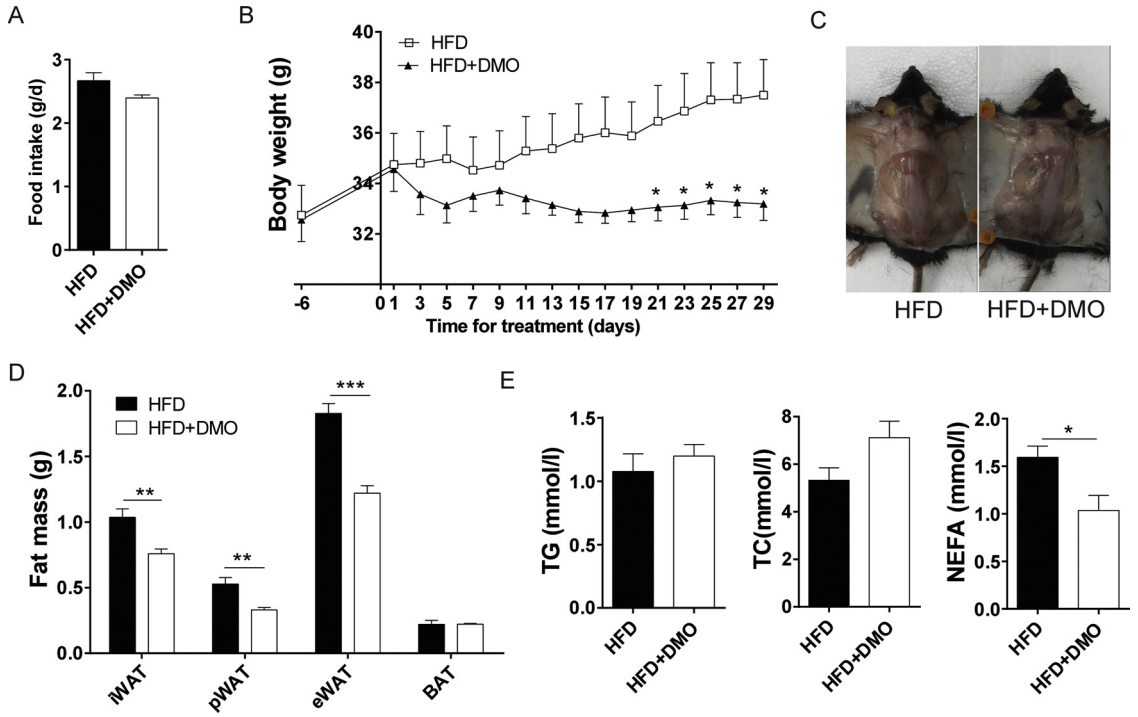

Fig. 2. Effect of DMO on body weight gain and adiposity in mice with high-fat diet. (A) Daily food intake of mice during the treatment with vehicle (HFD group) or DMO (HFD + DMO, 2 mg/kg, i.g.). (B) Body weight changes of mice during the 4 week treatment with vehicle or DMO. (C) Representative images of mice at sacrifice. (D) Weights of white adipose tissue (iWAT, pWAT, eWAT) and interscapular brown adipose tissue (BAT). (E) Serum level of total cholesterol (TC), triglyceride (TG) and non-esterified fatty acids (NEFA). Data are expressed as mean ± SEM, n = 5-7. Statistical analysis was performed using student's *t*-test (A, D, E) or two-way repeated-measures ANOVA (B); *p < 0.05, **p < 0.01, ***p < 0.001.

induced weight gain and hyperphagia are controversial (Horska et al., 2016, 2017; Lord et al., 2017). In our study, we did not observe any effect on food intake of obese mice after DMO treatment for 4 weeks (Fig.2A). Despite this, DMO-treated mice had much higher rectal temperature determined at their ambient environment, indicative of increased heat production after DMO treatment (Fig.5A, p < 0.05 by Student's *t*-test). To gain more insights, we examined the metabolic phenotype of mice individually housed in metabolic cages for 24 h.

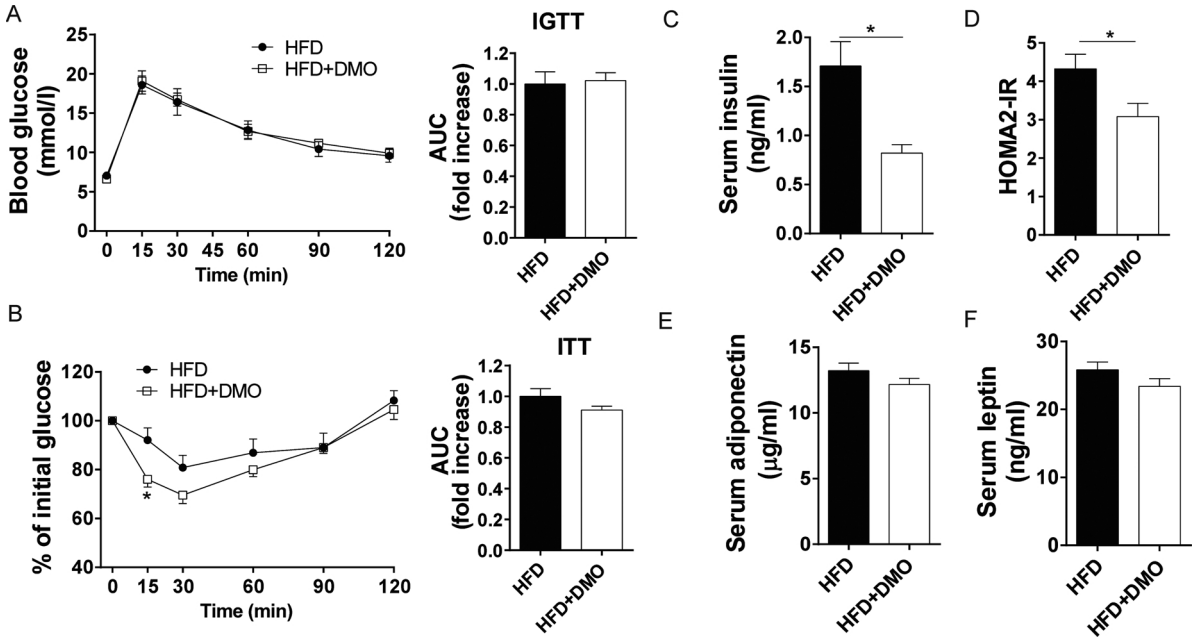

Fig. 3. Effects of OLA on glucose metabolism and insulin sensitivity in obese mice. (A) Blood glucose dynamics during the intraperitoneal glucose tolerance test (IGTT) after 4 h fasting and the area under the curve (AUC). (B) Blood glucose changes during the insulin tolerance test (ITT) and the AUC value. The data are expressed as percent of the baseline value. (C) Serum level of insulin in mice treated with DMO or vehicle for 4 weeks. (D) Homeostasis model assessment (version 2, HOMA2-IR) values based on fasting blood glucose concentration and serum insulin level. (E) Serum level of adiponectin. (F) Serum level of leptin. Values are expressed as mean ± SEM, n = 5–6. Statistical analysis was performed using student's *t*-test; for the blood glucose changes in (A,B), two-way repeated-measures ANOVA was used; *p < 0.05.

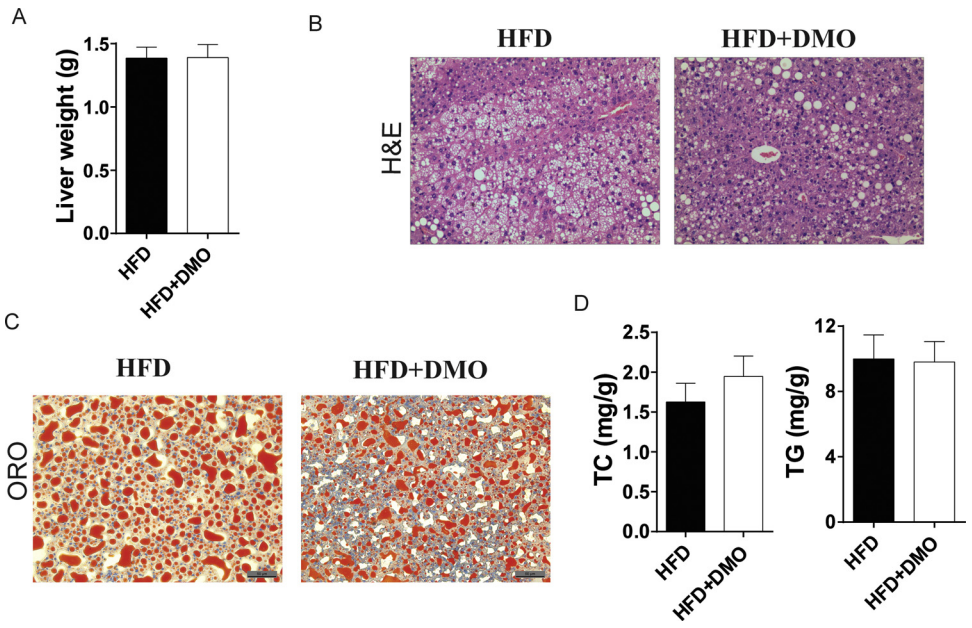

Fig. 4. Effect of OLA on liver steatosis and injury. (A) Liver weights of mice at the end of 12 weeks of HFD feeding. (B) Representative images of hematoxylin-eosin (H&E) staining of liver after 4 week treatment with DMO, scale bar: 50 μm. (C) Representative images of Oil Red O (ORO) staining of liver, scale bars: 50 μm. (D) Hepatic level of total cholesterol (TC) and total triglyceride (TG). Data are expressed as mean ± SEM, n = 5-7. Statistical analysis was performed using student's *t*-test (For interpretation of the references to colour in this figure legend, the reader is referred to the web version of this article).

DMO-treated mice exhibited significantly lower rates of oxygen consumption (VO_2; Fig.5B, $p < 0.001$ by two-way repeated-measures ANOVA) than the vehicle-treated counterparts during both light and dark cycles, while the rate of carbon dioxide production (VCO_2; Fig.5B, $p > 0.05$ by two-way repeated-measures ANOVA) did not differ between the two groups. In consistence, the respiratory exchange rate (RER), as indicated by $VCO_2/VO2$, was much higher in DMO-treated mice during all the light and dark phases, indicating an increased rate of energy metabolism after chronic DMO treatment (Fig.5C, $p < 0.0001$ by two-way repeated-measures ANOVA). Since the BAT is known as a major adipose tissue for energy expenditure, we further examined the change of BAT to understand the effect on energy metabolism. Of interest, histological examination revealed a marked difference in adipocyte morphology. It is evident that the BAT from DMO-treated mice has more abundant numbers of adipocytes, suggesting more functional capability for energy expenditure (Fig.5D). Taken together, these data suggest that energy metabolism of obese mice is increased after DMO treatment, which seems to play a role in the loss of body weight and fat mass.

3.5. DMO alleviates adipose dysfunction in mice

Dysfunctional adipose tissue is another hallmark of obesity and closely involved in insulin resistance and chronic inflammation (Friesen and Cowan, 2019). To gain more insights into the decreased adiposity after DMO treatment, we further examined the representative fat pads at histological and molecular levels. The representative WAT of HFD-induced obese mice, including the epididymal WAT (eWAT), inguinal WAT (iWAT) and perirenal WAT (pWAT), showed visibly enlarged adipocytes (Fig.6A), a typical marker of obesity. In contrast, much smaller adipocytes were readily found in the adipose tissue from DMO-treated mice (Fig.6A, B), especially those in the iWAT ($p < 0.0001$ by Student's *t*-test) and pWAT ($p < 0.0001$ by Student's *t*-test). Meanwhile, the appearance of small-diameter adipocytes interspersing in larger adipocytes is a typical morphology change that could be observed after DMO treatment, indicating increased potential for energy expenditure (Crane et al., 2015). In support of this functional potential, a significant increase of uncoupling protein 1 (UCP-1), a specialized mediator in energy use, was increased at the iWAT ($p < 0.05$ by Student's *t*-test) and pWAT ($p > 0.05$ by Student's *t*-test) after DMO treatment (Fig.6C). UCP-1 was undetectable in the eWAT.

Chronic inflammation in the adipose tissue is known to impede its function in maintaining energy balance. Of interest, quantitative PCR analysis of inflammatory mediators (*Il1β*, *Tnfα*, *e* and macrophage marker (*Cd68*) showed that DMO treatment had no appreciable effect on the mRNA expression of pro-inflammatory cytokines or macrophage markers in the iWAT or eWAT (Fig.6D). Among the inflammatory mediators, IL-1β is typically implicated in adipose dysfunction as a result of overt NLRP3 inflammasome activation (Swanson et al., 2019). We found that the mature form of IL-1β, which has a molecular weight of ˜17 kd, was markedly suppressed by DMO treatment in the iWAT (Fig.6E, $p < 0.05$ by Student's *t*-test). This finding indicates that DMO may suppress the production of active IL-1β in the WAT to improve its function in energy metabolism.

4. Discussion

Despite some knowledge on its neurobiological activity (David O Calligaro, 1997), direct effects of DMO on energy metabolism and neuroendocrine regulation are elusive. This knowledge gap may partially explain the fact that most studies exploring the metabolic effects of OLA are restricted to OLA itself. Such a commonly accepted view may underestimate the role of its metabolites, as suggested by our present findings. Our study here provides additional evidence on the metabolic and endocrinal impacts of DMO in a clinically relevant context. The regulatory effects of DMO on insulin resistance and energy expenditure, as well as the differential effects on liver and adipose tissue dysfunction, suggest the need to consider the contribution of DMO in understanding the metabolic responses to OLA therapy.

Metabolic adverse effect is a critical concern in the clinical use of AAPs such as OLA. To date, the biological determinants of this side effect remain incompletely understood, although several studies in animals have shown potential therapeutic strategies to counteract this problem (Lian et al., 2014; He et al., 2019). Our finding of the amelioration of metabolic disturbance by DMO is novel given that this is one of the major metabolites of OLA, which undergoes extensive metabolism after administration (Kassahun et al., 1997; Mattiuz et al., 1997). This raises a possibility that increasing DMO production from OLA may become a dual-targeting strategy to tackle the adverse metabolic effects with OLA therapy. Moreover, the beneficial effects of DMO on adipose inflammation and energy expenditure in obese mice suggest that the chemical scaffold of DMO may provide a novel template for the discovery of anti-obesity drugs. To this end, there is certainly much need to better understand the biological effects of DMO as well as the

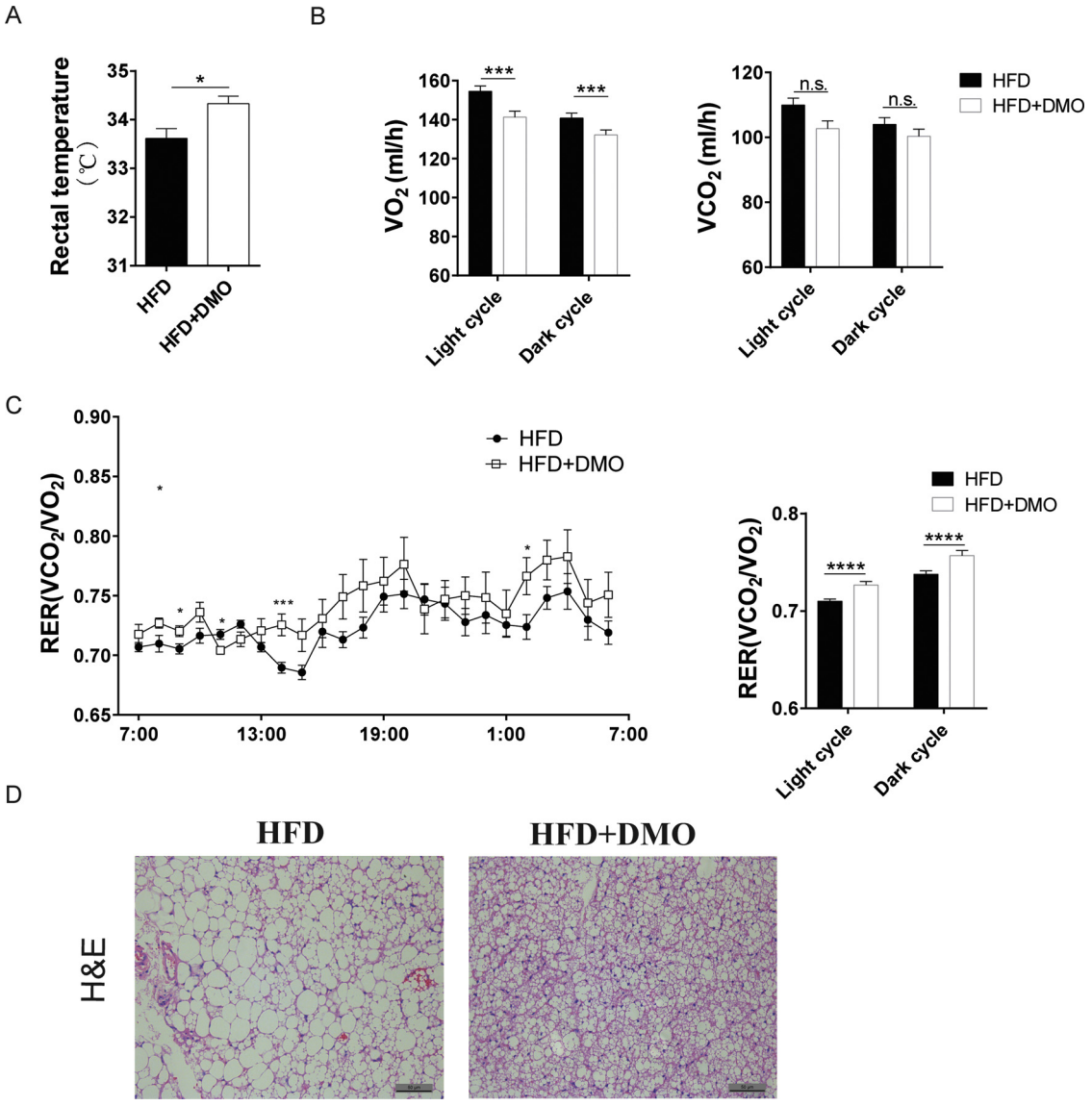

Fig. 5. Effect of OLA on energy expenditure in mice. (A) Rectal temperature of mice after 4 weeks of DMO treatment. The mice were housed at 25℃. (B) Oxygen consumption rate (VO_2) and carbon dioxide release rate (VCO_2) of mice over a 12 h light cycle and dark cycle. Mice were acclimated to metabolic cages for 24 h and data were collected for the next 24 h. (C) The respiratory exchange rate (RER) of mice, expressed as VCO2/VO2, over the light and dark cycle. (D) Representative H& E staining images of the BAT, scale bar: 50 μm. Data are expressed as mean ± SEM, n = 5-7. Statistical analysis was performed using student's *t*-test; the VO_2 and VCO_2 data and VCO_2/VO_2 in (B, C) were analyzed by two-way repeated-measures ANOVA; *p < 0.05, ***p < 0.001, ****p < 0.0001. n.s., no significant difference.

molecular mechanisms.

The antipsychotic effects of OLA are mechanistically linked to the antagonism of serotonin receptor (Htr), typically the Htr 2A/C and dopamine receptor D2 (Lukasiewicz et al., 2016). Central Htr 2A/C antagonism is proposed as a major mechanism to OLA-induced hyperphagia and weight gain (Lord et al., 2017). The contribution of peripheral modulation of Htr, however, remains largely unexplored. This is an essential consideration, given that peripheral inhibition of serotonin signaling has been shown to promote energy expenditure, partially *via* WAT browning and thermogenesis (Crane et al., 2015). These findings suggest that the metabolic outcome of AAPs could be better understood from Htr modulation in the brain and periphery and maybe determined by which target is preferably engaged (Horska et al., 2017). Of interest, DMO is reported to have antagonist effect on Htr such as Htr 2A *in vitro*, albeit with lower efficacy than OLA (David O Calligaro, 1997). However, its relatively higher polarity may shield it from an extensive engagement with central Htr. In this light, the opposite effect of central and peripheral serotonin system on energy metabolism might provide a novel perspective to understand the effect of DMO in counteracting obesity, as well as its difference to OLA in terms of metabolic regulation. Future studies are warranted to investigate, for example, whether the effects of DMO on adipose and hepatic pathology could be explained by the modulation of tissue-specific serotonin actions. Indeed, serotonin signals on the gut-liver axis and adipose tissue has been linked with liver steatosis and lipogenesis and thermogenesis in adipose tissue, respectively (Oh et al., 2015; Choi et al., 2018). Also, it would be of interest to test the metabolic action of other metabolites of OLA such as 2-hydroxymethyl-OLA, which was found at a higher concentration in female than male patients (Theisen et al., 2006).

Our findings that DMO could improve insulin resistance in the context of obesity has implications for clinical observations of variable metabolic outcome after OLA exposure. Firstly, previously studies have shown that factors such as gender and smoking habits are closely related to both the metabolic outcome and pharmacokinetic variability of

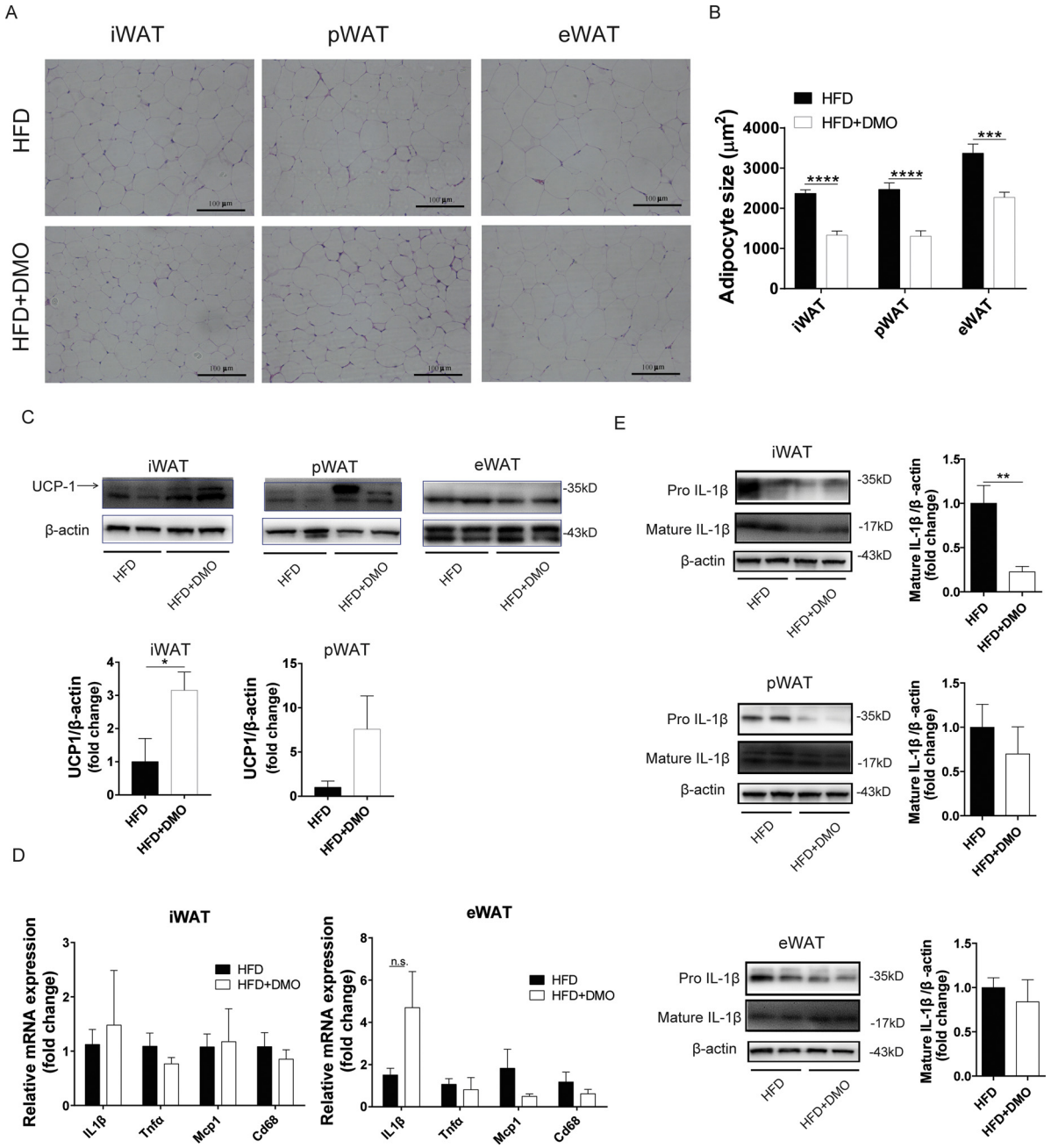

Fig. 6. Effect of OLA on adipose dysfunction in mice. (A) Representative H&E staining images of iWAT, pWAT and eWAT of mice. scale bar: 50 μm. (B) Average adipocyte sizes in the iWAT, pWAT and eWAT of mice were measured from H&E images using ImageJ software. (C) Representative Western blots of UCP-1 in the pWAT and eWAT of mice. The band with a molecular weight of ~35kd corresponds to UCP-1, which was undetectable in the eWAT. The relative expression of UCP-1 was normalized to that of β-actin (lower panel). (D) Relative gene expression of inflammatory mediators interleukin-1β (*Il1β*), tumor necrosis factor-α (*Tnfα*), monocyte chemoattractant protein-1 (*Mcp1*) and macrophage markers (cluster of differentiation 68, *Cd68*) in the iWAT (left panel) and eWAT (right panel). n.s., no significant difference. (E)Western blotting analysis of IL-1β precursor (~35 kD) and active form (~17 kD) in the iWAT, pWAT and eWAT of mice. The band with a molecular weight of 17kd corresponds to the mature form of IL-1β. The relative expression was normalized to that of β-actin. Data are expressed as mean ± SEM, n = 4-5. Statistical analysis was performed using student's *t*-test; *p < 0.05, **p < 0.01, ***p < 0.001, ****p < 0.0001.

OLA (Henderson et al., 2015; Polasek et al., 2018). Based on the results of our work, such a link maybe explained by the variable generation of DMO from OLA. Secondly, the concentration ratio between OLA and DMO was identified as positive predictor of adverse metabolic outcome in the clinic when it exceeded 6.3 (Lu et al., 2016). Given the direct metabolic impacts of DMO uncovered in our study, this may be explained from the perspective fact that DMO serves as an active metabolite of OLA that counteracts some of the metabolic adverse effects elicited by OLA. Therefore, therapeutic monitoring of OLA/DMO ratio in patients may serve as a rational predictor of the metabolic responses to OLA therapy, and it would be highly valuable to define a certain range which may help maximize the clinical efficacy and minimize the metabolic side effects.

The past decade has seen a great interest in understanding the metabolic response of AAPs in animal studies (Boyda et al., 2010). It is notable that female rats are preferably used in studies aiming to reproduce the metabolic side effects of OLA such as weight gain and metabolic disturbance. Indeed, the administration of OLA to male rats have been reported with inconsistent and largely negative findings (Boyda et al., 2010; van der Zwaal et al., 2014). Given the ameliorating

effects of DMO on weight gain, insulin resistance and adipose inflammation in obesity, as found in our present study, it would be reasonable to explore the gender-dependent metabolism of OLA to DMO in future studies. In fact, it has been reported that there is a high propensity of OLA metabolism to DMO in mice (Mattiuz et al., 1997). It is of interest to refer to our previous study in male mice that OLA administration to obese mice unexpectedly counteracted some parameters of metabolic disturbance, an effect that was not found in previous studies performed under normal conditions (Zhang et al., 2018) Collectively, these findings point to the need to verify and better understand the metabolic benefits of DMO in clinical settings.

To further strengthen the validity and clinical relevance of our study, several points are worthy of consideration in future studies. Firstly, housing temperature is an important consideration when measuring indices of non-shivering thermogenesis in mice, which have different thermal-neutral conditions (> 29 ℃) with humans. It was proposed that experiments with animals kept and examined at thermoneutrality are likely to yield findings for improving human metabolic disorder (Cannon and Nedergaard, 2011). Since in the present study the housing temperature is below this zone, further studies are needed to address the impact of DMO under thermal-neutral conditions. Secondly, only one dosage of DMO was examined in our present study. For a comprehensive understanding of the metabolic effects of DMO and assessment of clinical relevance, it is desirable to set additional dosage groups and observe the relationship between plasma concentrations of DMO and metabolic outcome. Lastly, the number of subjects per group in our study is relatively low, which may partially explain the absence of statistical significant differences in some parameters despite visible trends. Future studies are suggested to expand the number of mice to better understand the metabolic effects of DMO.

In summary, we found that, in the context of HFD-induced obesity, DMO could alleviate some parameters of metabolic disturbance, such as insulin resistance, adipose inflammation and decreased thermogenesis. To the best of our knowledge, this is the first time to investigate the pharmacology of DMO in conditions of metabolic disturbance in mice. Future assessment of the clinical relevance of these findings may provide useful insights to the metabolic changes induced by OLA and relevant AAPs. We believe that studies focusing on metabolic effects of OLA metabolites could give new impetus to optimize the clinical practice with these widely used antipsychotics.

Author contributions

X. Zhang and X. Zheng designed the research; X. Zhang, Y. Zhao and X. Zheng performed the research; Y. Zhao and X. Zhang analyzed the data; H. Shao and X. Zhang wrote the manuscript; X. Zhang and X. Zheng contributed to editing it.

Funding

This work was supported by the National Natural Science Foundation of China [grant number81503121] and Jiangsu Provincial Medical Youth Talent Project [grant number QNRC2016811].

Acknowledgements

We are grateful to Changle Zhu (Jiangsu Provincial Hospital of Chinese Medicine) for assistance with the histological analysis.

References

Aringhieri, S., Carli, M., Kolachalam, S., Verdesca, V., Cini, E., Rossi, M., McCormick, P.J., Corsini, G.U., Maggio, R., Scarselli, M., 2018. Molecular targets of atypical antipsychotics: from mechanism of action to clinical differences. Pharmacol. Ther. 192, 20–41.

Bobo, W.V., Cooper, W.O., Stein, C.M., Olfson, M., Graham, D., Daugherty, J., Fuchs, D.C., Ray, W.A., 2013. Antipsychotics and the risk of type 2 diabetes mellitus in children and youth. JAMA Psychiatry 70, 1067–1075.

Boyda, H.N., Tse, L., Procyshyn, R.M., Honer, W.G., Barr, A.M., 2010. Preclinical models of antipsychotic drug-induced metabolic side effects. Trends Pharmacol. Sci. 31, 484–497.

Cannon, B., Nedergaard, J., 2011. Nonshivering thermogenesis and its adequate measurement in metabolic studies. J. Exp. Biol. 214, 242–253.

Castberg, I., Westin, A.A., Skogvoll, E., Spigset, O., 2017. Effects of age and gender on the serum levels of clozapine, olanzapine, risperidone, and quetiapine. Acta Psychiatr. Scand. 136, 455–464.

Chang, J.C., Yen, A.M., Lee, C.S., Chen, S.L., Chiu, S.Y., Fann, J.C., Chen, H.H., 2013. A population-based cohort study to elucidate temporal relationship between schizophrenia and metabolic syndrome (KCIS no. PSY3). Schizophr. Res. 151, 158–164.

Choi, W., Namkung, J., Hwang, I., Kim, H., Lim, A., Park, H.J., Lee, H.W., Han, K.H., Park, S., Jeong, J.S., Bang, G., Kim, Y.H., Yadav, V.K., Karsenty, G., Ju, Y.S., Choi, C., Suh, J.M., Park, J.Y., 2018. Serotonin signals through a gut-liver axis to regulate hepatic steatosis. Nat. Commun. 9, 4824.

Crane, J.D., Palanivel, R., Mottillo, E.P., Bujak, A.L., Wang, H., Ford, R.J., Collins, A., Blumer, R.M., Fullerton, M.D., Yabut, J.M., Kim, J.J., Ghia, J.E., Hamza, S.M., Morrison, K.M., Schertzer, J.D., Dyck, J.R., Khan, W.I., Steinberg, G.R., 2015. Inhibiting peripheral serotonin synthesis reduces obesity and metabolic dysfunction by promoting brown adipose tissue thermogenesis. Nat. Med. 21, 166–172.

Daurignac, E., Leonard, K.E., Dubovsky, S.L., 2015. Increased lean body mass as an early indicator of olanzapine-induced weight gain in healthy men. Int. Clin. Psychopharmacol. 30, 23–28.

Davey, K.J., O'Mahony, S.M., Schellekens, H., O'Sullivan, O., Bienenstock, J., Cotter, P.D., Dinan, T.G., Cryan, J.F., 2012. Gender-dependent consequences of chronic olanzapine in the rat: effects on body weight, inflammatory, metabolic and microbiota parameters. Psychopharmacology (Berl.) 221, 155–169.

David O Calligaro, J., Hotten, Terrence M., Moore, Nicholas A., ETupper, David, 1997. The synthesis and biological activity of some known and putative metabolites of the atypical antipsychotic agent olanzapine (LY170053). Bioorg. Med. Chem. Lett. 7, 25–30.

Friesen, M., Cowan, C.A., 2019. Adipocyte metabolism and insulin signaling perturbations: insights from genetics. Trends Endocrinol. Metab. 30, 396–406.

He, M., Huang, X.F., Gao, G., Zhou, T., Li, W., Hu, J., Chen, J., Li, J., Sun, T., 2019. Olanzapine-induced endoplasmic reticulum stress and inflammation in the hypothalamus were inhibited by an ER stress inhibitor 4-phenylbutyrate. Psychoneuroendocrinology 104, 286–299.

Henderson, D.C., Vincenzi, B., Andrea, N.V., Ulloa, M., Copeland, P.M., 2015. Pathophysiological mechanisms of increased cardiometabolic risk in people with schizophrenia and other severe mental illnesses. Lancet Psychiatry 2, 452–464.

Horska, K., Ruda-Kucerova, J., Babinska, Z., Karpisek, M., Demlova, R., Opatrilova, R., Suchy, P., Kotolova, H., 2016. Olanzapine-depot administration induces time-dependent changes in adipose tissue endocrine function in rats. Psychoneuroendocrinology 73, 177–185.

Horska, K., Ruda-Kucerova, J., Karpisek, M., Suchy, P., Opatrilova, R., Kotolova, H., 2017. Depot risperidone-induced adverse metabolic alterations in female rats. J. Psychopharmacol. (Oxford) 31, 487–499.

Irwin, N., Gault, V.A., 2013. Unraveling the mechanisms underlying olanzapine-induced insulin resistance. Diabetes 62, 3022–3023.

Kassahun, K., Mattiuz, E., Nyhart Jr., E., Obermeyer, B., Gillespie, T., Murphy, A., Goodwin, R.M., Tupper, D., Callaghan, J.T., Lemberger, L., 1997. Disposition and biotransformation of the antipsychotic agent olanzapine in humans. Drug Metab. Dispos. 25, 81–93.

Lian, J., Huang, X.F., Pai, N., Deng, C., 2014. Betahistine ameliorates olanzapine-induced weight gain through modulation of histaminergic, NPY and AMPK pathways. Psychoneuroendocrinology 48, 77–86.

Lord, C.C., Wyler, S.C., Wan, R., Castorena, C.M., Ahmed, N., Mathew, D., Lee, S., Liu, C., Elmquist, J.K., 2017. The atypical antipsychotic olanzapine causes weight gain by targeting serotonin receptor 2C. J. Clin. Invest. 127, 3402–3406.

Lu, M.L., Chen, C.H., Kuo, P.T., Lin, C.H., Wu, T.H., 2018. Application of plasma levels of olanzapine and N-desmethyl-olanzapine to monitor metabolic parameters in patients with schizophrenia. Schizophr. Res. 193, 139–145.

Lu, M.L., Lin, C.H., Chen, Y.C., Yang, H.C., Wu, T.H., 2013. Determination of olanzapine and N-desmethyl-olanzapine in plasma using a reversed-phase HPLC coupled with coulochemical detection: correlation of olanzapine or N-desmethyl-olanzapine concentration with metabolic parameters. PLoS One 8, e65719.

Lu, M.L., Wu, Y.X., Chen, C.H., Kuo, P.T., Chen, Y.H., Lin, C.H., Wu, T.H., 2016. Application of plasma levels of olanzapine and N-Desmethyl-Olanzapine to monitor clinical efficacy in patients with schizophrenia. PLoS One 11, e0148539.

Lukasiewicz, S., Blasiak, E., Szafran-Pilch, K., Dziedzicka-Wasylewska, M., 2016. Dopamine D2 and serotonin 5-HT1A receptor interaction in the context of the effects of antipsychotics - in vitro studies. J. Neurochem. 137, 549–560.

Mattiuz, E., Franklin, R., Gillespie, T., Murphy, A., Bernstein, J., Chiu, A., Hotten, T., Kassahun, K., 1997. Disposition and metabolism of olanzapine in mice, dogs, and rhesus monkeys. Drug Metab. Dispos. 25, 573–583.

Musil, R., Obermeier, M., Russ, P., Hamerle, M., 2015. Weight gain and antipsychotics: a drug safety review. Expert Opin. Drug Saf. 14, 73–96.

Oh, C.M., Namkung, J., Go, Y., Shong, K.E., Kim, K., Kim, H., Park, B.Y., Lee, H.W., Jeon, Y.H., Song, J., Shong, M., Yadav, V.K., Karsenty, G., Kajimura, S., Lee, I.K., Park, S., 2015. Regulation of systemic energy homeostasis by serotonin in adipose tissues. Nat. Commun. 6, 6794.

Petersen, M.C., Shulman, G.I., 2018. Mechanisms of insulin action and insulin resistance. Physiol. Rev. 98, 2133–2223.

Polasek, T.M., Tucker, G.T., Sorich, M.J., Wiese, M.D., Mohan, T., Rostami-Hodjegan, A., Korprasertthaworn, P., Perera, V., Rowland, A., 2018. Prediction of olanzapine

exposure in individual patients using physiologically based pharmacokinetic modelling and simulation. Br. J. Clin. Pharmacol. 84, 462–476.
Swanson, K.V., Deng, M., Ting, J.P., 2019. The NLRP3 inflammasome: molecular activation and regulation to therapeutics. Nat. Rev. Immunol.
Theisen, F.M., Haberhausen, M., Schulz, E., Fleischhaker, C., Clement, H.W., Heinzel-Gutenbrunner, M., Remschmidt, H., 2006. Serum levels of olanzapine and its N-desmethyl and 2-hydroxymethyl metabolites in child and adolescent psychiatric disorders: effects of dose, diagnosis, age, sex, smoking, and comedication. Ther. Drug Monit. 28, 750–759.
Townsend, L.K., Peppler, W.T., Bush, N.D., Wright, D.C., 2018. Obesity exacerbates the acute metabolic side effects of olanzapine. Psychoneuroendocrinology 88, 121–128.
van der Zwaal, E.M., Janhunen, S.K., la Fleur, S.E., Adan, R.A., 2014. Modelling olanzapine-induced weight gain in rats. Int. J. Neuropsychopharmacol. 17, 169–186.
Wiebelhaus, J.M., Webster, K.A., Meltzer, H.Y., Porter, J.H., 2011. The metabolites N-desmethylclozapine and N-desmethylolanzapine produce cross-tolerance to the discriminative stimulus of the atypical antipsychotic clozapine in C57BL/6 mice. Behav. Pharmacol. 22, 458–467.
Yatham, L.N., Beaulieu, S., Schaffer, A., Kauer-Sant'Anna, M., Kapczinski, F., Lafer, B., Sharma, V., Parikh, S.V., Daigneault, A., Qian, H., Bond, D.J., Silverstone, P.H., Walji, N., Milev, R., Baruch, P., da Cunha, A., Quevedo, J., Dias, R., Kunz, M., Young, L.T., Lam, R.W., Wong, H., 2016. Optimal duration of risperidone or olanzapine adjunctive therapy to mood stabilizer following remission of a manic episode: a CANMAT randomized double-blind trial. Mol. Psychiatry 21, 1050–1056.
Zabala, A., Bustillo, M., Querejeta, I., Alonso, M., Mentxaka, O., Gonzalez-Pinto, A., Ugarte, A., Meana, J.J., Gutierrez, M., Segarra, R., 2017. A pilot study of the usefulness of a single olanzapine plasma concentration as an Indicator of early drug effect in a small sample of first-episode psychosis patients. J. Clin. Psychopharmacol. 37, 569–577.
Zhang, X., Zhao, Y., Liu, Y., Yuan, Y., Shao, H., Zheng, X., 2018. Regulation of obesity-associated metabolic disturbance by the antipsychotic drug olanzapine: role of the autophagy-lysosome pathway. Biochem. Pharmacol. 158, 114–125.